

Cite this: DOI: 10.1039/xxxxxxxxxx

Mass load effect on the the resonant acoustic frequencies of colloidal semiconductor nanoplatelets: Supplementary Information

Adrien Girard,^a Lucien Saviot,^b Silvia Pedetti,^c Mickaël D. Tessier,^c Jérémie Margueritat,^a Hélène Gehan,^a Benoit Mahler,^a Benoit Dubertret,^c and Alain Mermet*^a

Received Date

Accepted Date

DOI: 10.1039/xxxxxxxxxx

www.rsc.org/journalname

1 Raman measurements from CdS and CdSe NPLs

In order to enhance the low frequency Raman signal, nearly resonant excitation conditions were chosen with Raman excitations lying slightly above the hh exciton absorption edge. This choice is a compromise to guarantee an enhanced interaction with light through strong absorption with a somewhat minimum photoluminescence which tends to dominate the Raman spectra and thus hide the weaker low frequency Raman signals. Because of the operation constraints of the Raman spectrometers, several setups were used.

A multichannel micro-Raman HORIBA Labram HR spectrometer equipped with Notch filters operating at the fixed excitation wavelength of 532 nm was used for all CdS samples. Differently, the strong shift of the NPL excitonic edge for CdSe samples required to operate with a wavelength versatile macro setup built of a 5-grating monochromator equipped with single channel detection. The Raman spectra of the 3 ML, 4 ML, 5 ML and 11 ML CdSe NPLs were recorded with the 496.5 nm, 514.5 nm, 560 nm and 660 nm excitation lines respectively. The 6 ML CdSe NPL sample was investigated with a Renishaw Invia micro-spectrometer operating at 633 nm.

For several samples, it was checked that the Raman frequencies did not depend significantly upon wavelength excitation (Figure 1). For CdSe NPLs, the frequencies were deduced from the average values between 532 nm and 633 nm.

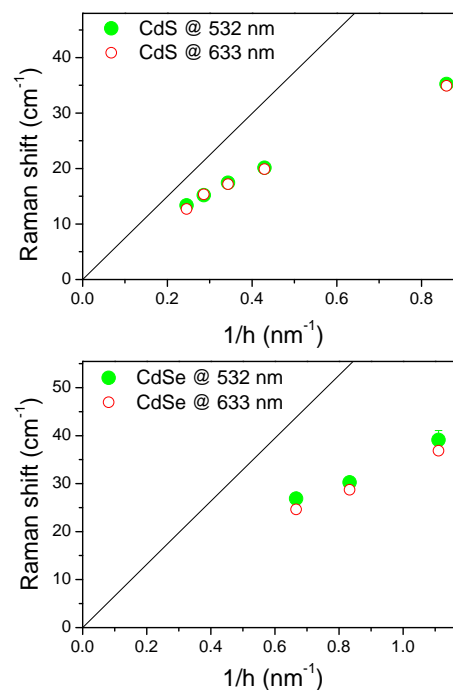


Fig. 1 Thickness mode frequency vs $1/h$ measured with 532 nm (full circles) and 633 nm (empty circles) excitation lines for selected CdS (top) and CdSe (bottom) NPL samples. No significant dependence upon wavelength excitation is observed. Lines are expected values from bare NPLs.

2 Determining C_{11} in Zinc-Blende CdS from quantum dots

Since bulk elastic constants of zinc-blende phase CdS and CdSe have, to our knowledge, not been characterized (available elastic data pertain essentially to the macroscopically stable wurtzite phase), we experimentally checked the value of $C_{11}^{ZB} = 98$ GPa

^a Institut Lumière Matière, Université de Lyon, Université Claude Bernard Lyon 1, UMR CNRS 5306, 69622 Villeurbanne, France

^b Laboratoire Interdisciplinaire Carnot de Bourgogne, UMR 6303 CNRS-Université de Bourgogne Franche Comté, 9 Av. A. Savary, BP 47 870, F-21078 Dijon Cedex, France

^c Laboratoire de Physique et d'Etudes des Matériaux, CNRS, Université Pierre et Marie Curie, ESPCI, 10 rue Vauquelin, 75005 Paris, France

* alain.mermet@univ-lyon1.fr

which was derived from ab-initio calculations¹ for bulk ZB-CdS. To this end, bare (i.e. ligand free) CdS quantum dots in the ZB phase were synthesized in order to measure, through low frequency Raman scattering, one known Lamb mode whose frequency depend on the value of C_{11}^{ZB} .

2.1 Synthesis of the bare ZB-CdS QDs

10 mL 1-octadecene (ODE) and 800 μ L Cd(oleate)₂ 0.5 M in oleic acid are introduced in a 100 mL three neck flask and degased for 30 min under vacuum at 70°C. Under Ar atmosphere, the temperature is raised to 250°C and 2 mL of S-ODE 0.1 M is swiftly injected. After 10 min annealing, half of the reaction mixture (5 mL) is taken out as sample 1. A stoichiometric mixture of S-ODE 0.1 M and Cd(oleate)₂ 0.5 M in oleic acid is then slowly injected (at 24 mL/h) and aliquots are taken at different times to obtain CdS nanocrystals samples of different sizes. The obtained nanocrystals samples have a mean sizes ranging from 4.8 nm to 7.2 nm diameter according to their absorption spectra² (Figure 2).

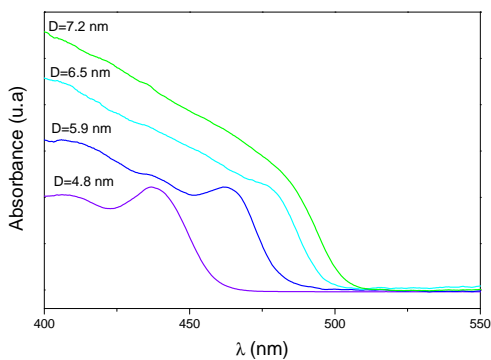


Fig. 2 Optical absorption spectra of bare ZB-CdS quantum dots with different diameters.

2.2 Raman measurements

The Raman measurements were performed in identical conditions as those described in the paper. Measurements were performed at 532 nm (using the HORIBA Labram HR micro-spectrometer) and at 633 nm (using the Renishaw Invia micro-spectrometer). Figure 3 displays the corresponding low frequency Raman spectra; once again, no dependence upon excitation wavelength is observed.

In accord with comparable measurements performed on CdS QDs embedded in glasses³, the prominent peaks are ascribed to the fundamental breathing Lamb modes (described by the angular momentum $\ell = 0$) of the quasi-spherical QDs. For bare spherical nanoparticles, the Lamb $\ell = 0$ mode frequency is given by:

$$v_{\ell=0} \simeq 0.9 \frac{V_L}{D} = \frac{0.9}{D} \sqrt{\frac{C_{11}}{\rho}} \quad (1)$$

A linear fit of the experimental frequencies (Figure 3- bottom) along this equation yields $C_{11}^{ZB-CdS} = 98$ GPa ($\rho_{ZB-CdS} = 4870$ kg.m⁻³). This value is in excellent agreement with that derived from ab-initio calculations¹.

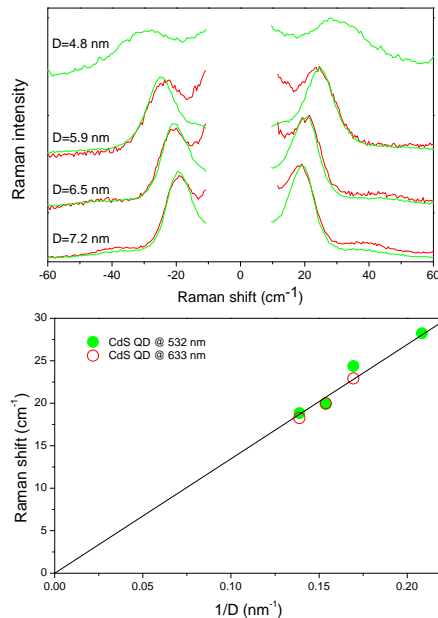


Fig. 3 Top : Low frequency Raman spectra of bare CdS quantum dots recorded with two different excitation wavelengths, 532 nm (green lines) and 633 nm (red lines). Indicated sizes are diameters. Bottom : Frequency dependence of reciprocal diameter $1/D$. The line is a zero intercept fit along Equation 1, yielding $C_{11}^{CdS} = 98 \pm 2$ GPa.

3 Analysis of published Raman data from MoS₂ and WSe₂ nanosheets⁴

Zhao *et al*⁴ recently reported low frequency Raman measurements from MoS₂ and WSe₂ nanosheets with thicknesses lying between 1 and 6 nm. Compared to our colloidal NPLs, these systems have no ligands. Among the detected low frequency modes, two of them (named *B1* and *B2* in Ref.⁴) show frequencies decreasing with increasing thickness. DFT calculations⁴ helped assign these modes to the fundamental and third overtone of so-called interlayer breathing modes. These modes are in fact thickness breathing modes, along the descriptions in Figure 4 of Ref.⁴. Accordingly, plotting the fundamental *B1* frequencies of MoS₂ and WSe₂ nanosheets as a function of the corresponding reciprocal nanosheet thicknesses* (bottom graph of Figure 2 in the paper), one observes linear trends as expected from Equation 1 of the paper. Linear fits of these data yield, using macroscopic densities[†], C_{33} values of 55 ± 2 GPa and 51 ± 1 GPa for MoS₂ and WSe₂ respectively (note that differently from cubic structures, the speed of sound in such hexagonal close packed structures along the thickness direction is given by $\sqrt{\frac{C_{33}}{\rho}}$). These values perfectly match the C_{33} values derived from the mass-spring model developed in Ref.⁴.

* using 0.675 nm and 0.67 nm as one trilayer thickness in MoS₂ and WSe₂ respectively⁵

† i.e. 5.06 kg.m⁻³ and 9.32 kg.m⁻³ for MoS₂ and WSe₂ respectively

4 Evaluation of the influences of the parameters C_{11} , ρ and σ on the NPL frequencies

Figure 4 displays the separate dependencies of the lumped mass frequencies for CdS NPLs on the input parameters C_{11} , ρ and σ , i.e. changing one of the three parameters while fixing the two other ones at their nominal values ($C_{11}^{\text{ZB-CdS}} = 98$ GPa, $\rho_{\text{ZB-CdS}} = 4870$ kg.m⁻³ and $\sigma_{\text{OA}}^{\text{CdS}} = 5.9$ OA/nm²). The results are com-

mented in the main paper.

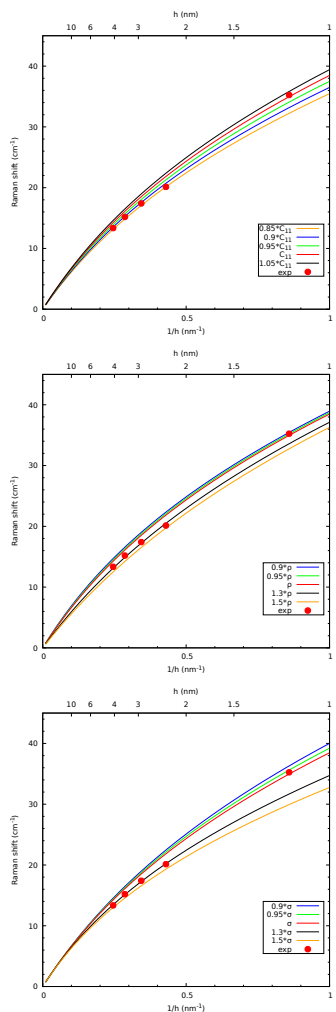


Fig. 4 Lumped mass frequencies for CdS NPLs changing C_{11} only (top), ρ only (middle) and σ only (bottom).

References

- 1 E. Deligoz, K. Colakoglu and Y. Ciftci, *Physica B: Condensed Matter*, 2006, **373**, 124–130.
- 2 W. W. Yu, L. Qu, W. Guo and X. Peng, *Chem. Mater.*, 2003, **15**, 2854–2860.
- 3 L. Saviot, B. Champagnon, E. Duval and A. I. Ekimov, *Phys. Rev. B*, 1998, **57**, 341–.
- 4 Y. Zhao, X. Luo, H. Li, J. Zhang, P. T. Araujo, C. K. Gan, J. Wu, H. Zhang, S. Y. Quek, M. S. Dresselhaus and Q. Xiong, *Nano Letters*, 2013, **13**, 1007–1015.
- 5 M. M. Benameur, B. Radisavljevic, J. S. Heron, S. Sahoo, H. Berger and A. Kis, *Nanotechnology*, 2011, **22**, 125706.